This article has been accepted for publication in a future issue of this journal, but has not been fully edited. Content may change prior to final publication. Citation information: DOI 10.1109/TII.2019.2903267, IEEE Transactions on Industrial Informatics

# Fault Location Method in Power Network by Applying Accurate Information of Arrival Time Differences of Modal Traveling Waves

Rui Liang, *Member, IEEE,* Nan Peng, *Student Member, IEEE,* Lutian Zhou, Xiangzhen Meng, Yihua Hu, *Senior Member, IEEE,* Yaochun Shen, and Xue Xue

***Abstract*—Faults may be generated in power networks as a result of bad weather, human activities or some other factors. The complex structure of power network adds to the difficulty of fault location (FL). This paper presents a novel FL scheme by utilizing the information of the time differences of arrival (TDOAs) of modal traveling waves (MTWs) asynchronously sampled in the network. First, the fault area is determined by searching the minimum TDOA of MTWs. Then, by applying the fictitious fault point method in the fault area, the minimum accumulated difference is used to detect the fault line. Finally, the accurate FL is estimated by solving the objective function of the absolute distance between the FL and multiple FL candidates. Various simulations are carried out in IEEE 30-bus system. The calculation results demonstrate that the method is not affected by fault impedance, inception angle, location and noises to a certain extent.**

***Index Terms*—time difference of arrival, modal traveling wave, asynchronous measurement, fault location, power network.**

## I. INTRODUCTION

WITH the increasing scale of power grids, the possibility of faults in power lines is growing. For distribution networks, fault line detection is a traditional but tough task [1]. Similar to distribution networks, wide-area protection [2] in transmission networks aims to correctly, reliably and quickly detect the fault line, which plays an important role. However, protection in transmission networks is insufficient for fast maintenance due to long transmission distance. Fast and accurate FL for power network is of great significance for reducing economic losses and improving system reliability [3].

Many FL methods, having shown promising performance, have been devoted to locating faults in power network. These methods can be mainly divided into two categories: impedance based methods [4] and traveling wave based methods [5-7]. Traveling wave based methods usually utilize the arrival time stamps of the first or subsequent wave fronts at one terminal or double terminals to locate faults in transmission lines [8].

In recent years, signal processing, communication technology and wide-area measurement have witnessed tremendous and rapid progress, expediting new development of traveling wave based FL methods in high-voltage power networks. The methods in [9-10] acquire the arrival time of the voltage travelling waves to locate faults in wide-area power network. Still in [11], an accurate FL method for multi-terminal transmission systems using the current travelling waves is proposed. Actually most FL methods require accurate synchronous measurement [12-13]. Based on least-absolute-value estimation, the method in [13] exploits the automatic bad-data rejection property of the FL estimators.

Considering the fault occurrence time, a method using the arrival time of the traveling waves measured by traveling wave recorders (TWRs) is presented in [14]. The method introduces Manhattan Distance to find the preliminary FL and improves the final FL accuracy by error compensation. The methods in [15-16] only utilize the arrival time information of the traveling waves acquired at only a few TWRs in the power network to reduce the measurement cost. In addition, an extended FL method based on IEC61850 that supports open communication and interoperability between measurement equipment and station, is proposed in [17]. Based on speed-up robust features, the method in [18] divides the initial signal window into two inconsistent time windows to simply identify the initial and reflected traveling wave fronts. Considering the shortest propagation paths of traveling waves, the method in [19] uses the multi-level data fusion of MTWs to realize FL.

Although many FL methods have been developed to locate faults in high-voltage power networks, some of them [11-13]

Manuscript received October 1, 2018; revised January 15, 2019; accepted February 24, 2019. Date of publication September 18, 2017; date of current version April 3, 2018. This work is supported by the Fundamental Research Funds for the Central Universities 2017XKQY033. (Corresponding author: Rui Liang.)

Rui Liang, Nan Peng, Lutian Zhou, Xiangzhen Meng are with the School of Electrical and Power Engineering, China University of Mining and Technology, Xuzhou, 221116, China (e-mail: liangrui@cumt.edu.cn; pncumt@163.com; zhoulutian@hotmail.com; 974776496@qq.com).

Yihua Hu and Yaochun Shen are with the Department of Electrical Engineering and Electronics, University of Liverpool, Liverpool L69 3GJ, U.K. (e-mail: y.hu35@liverpool.ac.uk; y.c.shen@liverpool.ac.uk).

Xue Xue is with the School of Information and Control Engineering, China University of Mining and Technology, Xuzhou, 221116, China (e-mail: cumtxx@126.com).

This article has been accepted for publication in a future issue of this journal, but has not been fully edited. Content may change prior to final publication. Citation information: DOI 10.1109/TII.2019.2903267, IEEE Transactions on Industrial Informatics

require strict time synchronization, and others [9, 14] may have large errors in practice due to inaccurate detection of WFs with noise interference, and the rest of them [15-16] do not consider the near-bus fault. To over the shortcomings, this paper presents a novel FL method for transmission networks. In the method, the arrival time differences of the modal traveling waves are utilized to locate the faults, which does not require accurate synchronization. Combining the advantages of wavelet transform and Teager energy, the wavelet Teager energy algorithm is presented to detect the traveling wave fronts with noise interference. To improve the FL accuracy with near-bus fault, by applying the fictitious point method and simplified TDOA ratio formula, the defined accumulated equivalent absolute difference between the calculated and theoretical TDOA acquired at multiple buses is computed to estimate the accurate FL.

The main contributions of this paper are presented as follows. Firstly, a fast and simple fault area determination criterion using actual TDOA of the asynchronously sampled MTWs is presented. Secondly, based on the fictitious fault point method, the TDOA at each selected pair of the buses is used to construct the FL objective function, which is applicable to both general and near-bus faults. Thirdly, considering the shortest propagation path of traveling waves, a simplified calculation formula of TDOA ratio is proposed to reduce the computational burden. Fourthly, compared with the state-of-the-art methods, the proposed scheme has the advantages of asynchronous measurement, high accuracy for both general and near-bus faults and great sensitivity to various fault conditions and noises.

The remainder of this paper is organized as follows. The complete FL scheme is described in section II, where fault area determination and accurate FL are shown in two subsections. The details of FL scheme implementation are provided in section III. In this section, the wave front detection method, simplified formula for computing TDOA ratio and searching algorithm for solving FL objective function are presented in three subsections. The simulation test, related FL calculation results and discussions are presented in section IV. Section V draws the conclusions.

## II. FL SCHEME BASED ON TDOA OF MTWS

When a fault occurs in a transmission network, the fault generated MVTWs propagate along the lines, reflect and refract at bus nodes. Due to attenuation, the decrease of the velocity of zero-mode traveling wave with propagation distance is more significant than that of the aerial-mode traveling wave. Thus, the TDOA information of the MTWs measured at the buses varies with the propagation paths of traveling waves that are determined by the FL. The TDOA of MTWs is related to the FL. In general, the shorter the distance between the actual FL and measurement point, the smaller the TDOA of MVTWs. In this paper, the TDOA information is fully used to pinpoint the fault in the transmission network.

### A. Fault Area Determination

After a fault is detected in the power network, the calculated TDOA of the MTWs measured at bus $n$ can be expressed by

$$\Delta t_{n\_cal} = t_{z\_n} - t_{a\_n} \tag{1}$$

where $\Delta t_{n\_cal}$ is the TDOA at bus $n$. $t_{a\_n}$ and $t_{z\_n}$ represent the actual arrival time stamps of the aerial- and zero-mode traveling waves recorded at bus $n$ respectively. According to (1), the actual TDOA array of the MTWs propagating in the whole network is constructed as

$$T_{\Delta} = [\Delta t_{1\_cal}, \Delta t_{2\_cal}, ..., \Delta t_{N\_cal}] \tag{2}$$

In (2), $T_{\Delta}$ is the actual TDOA array and $N$ is the total number of the mounted measurement devices. The bus corresponding to the minimum element in $T_{\Delta}$ must be closest to the actual fault point. Thus, the bus of the nearest fault line to the actual FL can be determined by

$$N_f = \min_n (T_{\Delta}) \tag{3}$$

where $N_f$ is the bus number corresponding to the minimum element in $T_{\Delta}$. The fault area contains all the lines connecting to bus $N_f$.

### B. Accurate Fault Location

In traditional accurate FL practice, only the arrival time information of the traveling waves recorded at both terminal buses of the fault line is used [19]. The value of the time-domain information of the traveling waves recorded at the neighboring buses is not fully excavated. In fact, the TDOA information of the MVTWs acquired at the buses of the fault line and their adjacent buses helps improve the FL accuracy. Thus, the proposed accurate FL method takes full advantage of the TDOA information of the MVTWs measured at multiple buses in the determined fault area.

A typical topology of a fault area (in IEEE 30-bus test system) is depicted in Fig.1. In the figure, one bus node of the fault line is bus $N_f$ and the other is bus $N_c$. F is the actual fault point. $N_f$ is assumed to be the bus that is closest to F. Since F is close to $N_f$, the TDOA information at $N_f$ may not be accurately acquired, which increases the FL error.

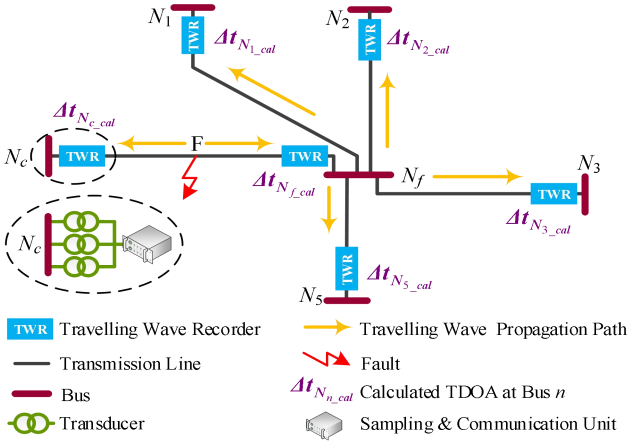


Fig.1 Diagram of a typical determined fault area

This article has been accepted for publication in a future issue of this journal, but has not been fully edited. Content may change prior to final publication. Citation information: DOI 10.1109/TII.2019.2903267, IEEE Transactions on Industrial Informatics

Considering all the buses except bus $N_f$ in the determined fault area, for any line section $L_{NiNj}$ (in Fig.1, $i$ and $j$={1, 2, 3, 5, $c$}) (the line section between bus $N_i$ and bus $N_j$, including the lines $L_{NiNf}$ and $L_{NfNj}$) in the determined fault area, if a fault is assumed to occur at a fictitious point $F_f$ in the line between bus $N_i$ and bus $N_f$ (Line $L_{NiNf}$), the theoretical TDOA of the MTWs measured at bus $N_i$ and bus $N_j$ can be formulated by

$$\begin{cases} \Delta t_{N_i\_fic}\left(x_{N_iF_f}\right)=\dfrac{P_{F_f\to N_i}\left(x_{N_iF_f}\right)\cdot\left(v_1-v_0\right)}{v_1\cdot v_0} \\ \Delta t_{N_j\_fic}\left(x_{N_iF_f}\right)=\dfrac{P_{F_f\to N_j}\left(x_{N_iF_f}\right)\cdot\left(v_1-v_0\right)}{v_1\cdot v_0} \end{cases} \tag{4}$$

where $x_{NiFf}$ is the distance between $F_f$ and bus $N_i$. $\Delta t_{Ni\_fic}$ ($x_{NiFf}$) and $\Delta t_{Nj\_fic}$ ($x_{NiFf}$) are the TDOAs of the MTWs at bus $N_i$ and bus $N_j$ corresponding to $x_{NiFf}$. $P_{Ff\to Ni}$ ($x_{NiFf}$) is the shortest path between $F_f$ and $N_i$. $P_{Ff\to Nj}$ ($x_{NiFf}$) is the shortest path between $F_f$ and $N_j$. $v_1$ and $v_0$ are the wave velocities of the aerial- and zero-mode traveling waves, respectively.

According to (4), a TDOA ratio can be derived as

$$R_{N_iN_j\_fic}\left(x_{N_iF_f}\right)=\frac{\Delta t_{N_i\_fic}\left(x_{N_iF_f}\right)}{\Delta t_{N_j\_fic}\left(x_{N_iF_f}\right)}=\frac{P_{F_f\to N_i}\left(x_{N_iF_f}\right)}{P_{F_f\to N_j}\left(x_{N_iF_f}\right)} \tag{5}$$

where $R_{NiNj\_fic}$ ($x_{NiFf}$) is the ratio of $\Delta t_{Ni\_fic}$ ($x_{NiFf}$) to $\Delta t_{Nj\_fic}$ ($x_{NiFf}$). The calculated TDOA of the MTWs measured at bus $N_i$ and bus $N_j$ are denoted as $\Delta t_{Ni\_cal}$ and $\Delta t_{Nj\_cal}$ respectively. The calculated TDOA ratio can be then obtained by

$$R_{N_iN_j\_cal}=\frac{\Delta t_{N_i\_cal}}{\Delta t_{N_j\_cal}} \tag{6}$$

where $R_{NiNj\_cal}$ represents the ratio of $\Delta t_{Ni\_cal}$ to $\Delta t_{Nj\_cal}$. Based on (5) and (6), the absolute difference between $R_{NiNj\_fic}$ ($x_{NiFf}$) and $R_{NiNj\_cal}$ is expressed by

$$d_{N_iN_j}\left(x_{N_iF_f}\right)=\left|R_{N_iN_j\_fic}\left(x_{N_iF_f}\right)-R_{N_iN_j\_cal}\right|=\left|\frac{P_{F\to N_i}\left(x_{N_iF_f}\right)}{P_{F\to N_j}\left(x_{N_iF_f}\right)}-\frac{\Delta t_{N_i\_cal}}{\Delta t_{N_j\_cal}}\right| \tag{7}$$

In (7), $d_{NiNj}$ ($x_{NiFf}$) is the absolute difference when the fictitious fault point $F_f$ is $x_{NiFf}$ away from the terminal $N_f$. From the starting point of line section $L_{NiNj}$, a fault is sequentially assumed to occur at each fictitious point along the line between bus $N_i$ and bus $N_f$ with a fixed distance step $\Delta x$. Then, an absolute difference array $D_{NiNj}$ can be obtained as

$$D_{N_iN_j}=\left[d_{N_iN_j}(0),\, d_{N_iN_j}(\Delta x),\, d_{N_iN_j}(2\cdot\Delta x),\ldots,\, d_{N_iN_j}(M\cdot\Delta x)\right] \tag{8}$$

where $M$ is the total number of all the fictitious fault points along the line between bus $N_i$ and bus $N_f$.

Accurate extraction of the arrival time of traveling waves is crucial to accurate FL. Considering the error of the arrival time of zero-mode traveling wave, the actual ratio defined in (6) can be expressed as

$$R_{N_iN_j\_cal}=\left[\frac{\Delta t_{N_i\_cal}\pm t_{Err}}{\Delta t_{N_j\_cal}\pm t_{Err}}\right] \tag{9}$$

where $t_{Err}$ represents the time error. In this paper, $t_{Err}$ is 1μs with 1MHz sampling frequency. It can be observed that $R_{NiNj\_cal}$ shown in (9) is a vector with 9 elements. As for each element in $R_{NiNj\_cal}$, an absolute difference array can be calculated according to (5)-(8).

If the absolute difference array for the $k$th element in $R_{NiNj\_cal}$ is denoted as $D_{NiNj\_k}$, the criterion for fault line detection can be defined as

$$\begin{cases} \min\limits_i\left(D_{N_i\_acc\_equ}\right) \\ D_{N_i\_acc\_equ}=\begin{cases}\sum\limits_j \min\left(\dfrac{1}{9}\sum\limits_{k=1}^{9}\left(D_{N_iN_j\_k}\right)\right), & j\neq i \\ 0, & j=i\end{cases} \end{cases} \tag{10}$$

where $D_{Ni\_acc\_equ}$ is the accumulated equivalent absolute difference of the line section between buses $N_i$ and $N_j$. It is indicated in (10) that the other bus of the fault line corresponds to the minimum $D_{Ni\_acc\_equ}$.

After detecting the fault line, multiple FLs can be obtained by searching the minimum element in the corresponding absolute difference array of the fault line. Among all the obtained FLs, the minimum value $x_{c\_min}$ and maximum value $x_{c\_max}$ can be determined by

$$\begin{cases} x_{c\_min}=\min\limits_k\left(\min\left(D_{N_cN_j\_k}\right)\right) \\ x_{c\_max}=\max\limits_k\left(\min\left(D_{N_cN_j\_k}\right)\right) \end{cases} \tag{11}$$

If the actual fault point F is very close to $N_f$, the TDOA information acquired at $N_f$ should be discarded and that at the adjacent buses can be fully utilized. If not, the TDOA information obtained at $N_f$ and other adjacent buses should be used. To determine whether the TDOA of the MTWs measured at $N_f$ can be used in accurate FL, a criterion is defined by

$$\begin{cases} \left|L_F-x_{c\_max}\right|<l_{th}\ ,\ \Delta t_{N_f\_cal}\ \text{cannot be used} \\ \left|L_F-x_{c\_max}\right|\geq l_{th}\ ,\ \Delta t_{N_f\_cal}\ \text{can be used} \end{cases} \tag{12}$$

where $\Delta t_{Nf\_actual}$ is the actual TDOA at bus $N_f$. $L_F$ is the length of the detected fault line. $l_{th}$ is the distance threshold that is used to judge whether the fault point $F$ is close to $N_f$. In this paper, $l_{th}$ is set as 5km based on minimum identified TDOA with 1MHz sampling frequency.

If $\Delta t_{Nf\_actual}$ is used, the fictitious fault point method shown in (4)-(10) can be applied to the detected fault line by using the TDOA of the MTWs recorded at buses $N_c$ and $N_f$. Since the actual fault point is close to the all the obtained FLs, the objective function of estimating the actual FL can be constructed as:

$$\begin{aligned} &f\left(x_F\right)=\sum_{k,j}\left|x_F-\min\left(D_{N_cN_j\_k}\right)\right| \\ &st.\qquad x_{c\_min}\leq x_F\leq x_{c\_max} \end{aligned} \tag{13}$$

This article has been accepted for publication in a future issue of this journal, but has not been fully edited. Content may change prior to final publication. Citation information: DOI 10.1109/TII.2019.2903267, IEEE Transactions on Industrial Informatics

In (13), $f(\cdot)$ is the objective function. $x_F$ is the fault distance variable. $x_{c\_min}$ and $x_{c\_max}$, determined by (11), are the minimum and maximum FL candidates, respectively. By solving (13), the accurate FL can be achieved.

## III. IMPLEMENTATION OF THE FL SCHEME

Fig.2 displays the implementation steps of the proposed FL scheme. There are two stages of conducting the FL scheme. The details are as follows.

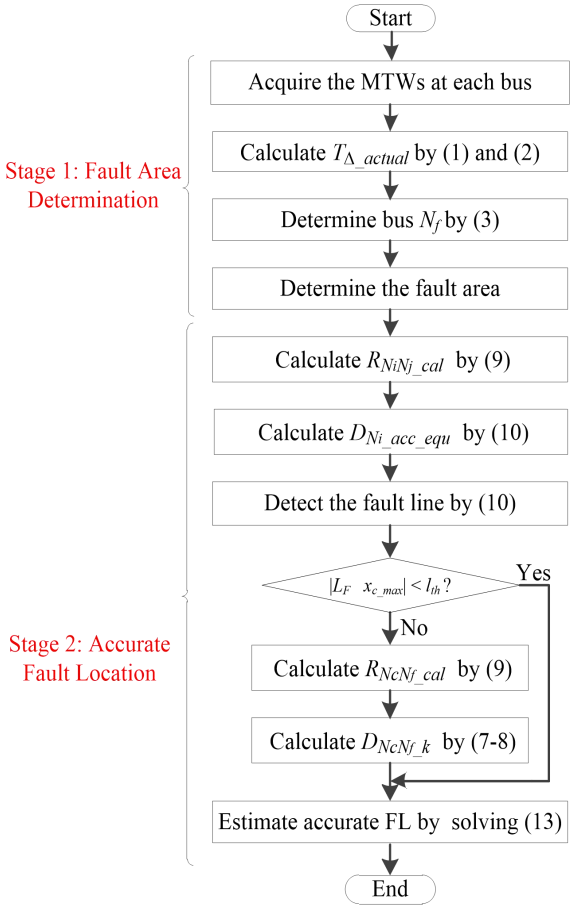


Fig.2 The flowchart of the FL scheme

◆*Stage* 1: *Fault Area Determination*

First, the MTW signals are sampled at all the buses in the power network. Next, by applying the wavelet Teager energy algorithm to the acquired signals, the arrival time of the MTW at each bus is determined. Then, the TDOA at each bus is calculated according to (1). Finally, according to (3), the bus closest to the fault is determined. The fault area consists of all the lines connecting to this bus.

◆*Stage* 2: *Accurate Fault Location*

First, as for each line section in the fault area, from the local bus to the bus that is closest to the fault, the calculated TDOA ratio $R_{NiNj\_fic}$ ($x_{NiFf}$) at each fictitious fault point is estimated by using the simplified formula shown in (14)-(17). Next, the absolute difference (denoted as $D_{NiNj\_k}$) between $R_{NiNj\_fic}$ and the actual one $R_{NiNj\_cal}$ shown in (9) is calculated for each point. Then, the absolute difference mentioned above is computed for each line section. Finally, the fault line is determined by criterion (10). Based on the objective function in (13), the accurate FL is estimated by using the $D_{NiNj\_k}$ corresponding to the fault line.

It can be observed that the extraction of the arrival time of MTWs, calculation of the theoretical ratio and solution to the FL objective function are the key parts in the implementation of FL scheme. The details are described in the following subsections.

### A. *Arrival Time Acquisition of MTWs by Wavelet Teager Energy Method*

Teager energy operator is nonlinear, which can effectively reflect the dramatic variations of signal amplitude, frequency, and instantaneous energy [11]. In this paper, discrete wavelet transform and Teager energy operators are organically combined to acquire the arrival time of the MTW signals, which shows better performance than single wavelet transform with noises. The detailed steps of the method are as follows: (1) Acquire the MTW at each bus. (2) Apply 4-layer db6 wavelet decomposition to the acquired signal and extract detailed coefficients of $d_1$ level. (3) Conduct wavelet reconstruction of the detailed coefficients. (4) Calculate the wavelet Teager energy $\Psi_e$ of the obtained reconstruction coefficients and eliminate the edge effect. (5) Acquire the arrival time stamp with respect to the modal maximum value of $\Psi_e$.

### B. *Simplified Calculation Formulas of the Calculated Ratio* $R_{NiNj\_fic}$

In accurate FL, the calculation of $R_{NiNj\_fic}$ can be time-consuming if the shortest path algorithm (such as Dijkstra, Floyd and Bellman-ford algorithms) is applied for each fictitious fault point in each line section. To reduce computational burden, the simplified calculation formulas for computing $R_{NiNj\_fic}$ are presented.

As for the fault area in Fig.1, three basic topologies– triangle, loop and radial topologies (shown in Fig.3) – can be identified before conducting accurate FL. In the following analysis, $l_{NiNj}$ denotes the length of the line between buses $N_i$ and $N_j$. It is assumed that the distance between the fictitious fault point and bus $N_f$ is $x_{Nf}$. Due to space limitation, only the formulas for triangle topology are elaborated. The theoretical ratio can be easily determined by the following formulas.

If $l_{N1Nc} + l_{NcNf} > l_{N1Nf}$ and $l_{N1Nc} + l_{N1Nf} < l_{NcNf}$, then we have:

$$R_{N_cN_1\_fic}\left(x_{N_f}\right)=\frac{\Delta t_{N_c\_fic}\left(x_{N_f}\right)}{\Delta t_{N_1\_fic}\left(x_{N_f}\right)}=\begin{cases}\dfrac{x_{N_f}+l_{N_1N_f}+l_{N_1N_c}}{x_{N_f}+l_{N_1N_f}}, & 0\le x_{N_f}\le\dfrac{l_{N_cN_f}-l_{N_1N_f}-l_{N_1N_c}}{2}\\ \dfrac{l_{N_cN_f}-x_{N_f}}{x_{N_f}+l_{N_1N_f}}, & \dfrac{l_{N_cN_f}-l_{N_1N_f}-l_{N_1N_c}}{2}<x_{N_f}\le\dfrac{l_{N_cN_f}-l_{N_1N_f}+l_{N_1N_c}}{2}\\ \dfrac{l_{N_cN_f}-x_{N_f}}{l_{N_cN_f}-x_{N_f}+l_{N_1N_c}}, & \dfrac{l_{N_cN_f}-l_{N_1N_f}+l_{N_1N_c}}{2}<x_{N_f}\le l_{N_cN_f}\end{cases}\quad(14)$$

Else if $l_{N1Nc} + l_{NcNf} > l_{N1Nf}$ and $l_{N1Nc} + l_{N1Nf} \ge l_{NcNf}$, then we have:

This article has been accepted for publication in a future issue of this journal, but has not been fully edited. Content may change prior to final publication. Citation information: DOI 10.1109/TII.2019.2903267, IEEE Transactions on Industrial Informatics

$$R_{N_cN_1\_fic}\left(x_{N_f}\right)=\frac{\Delta t_{N_c\_fic}\left(x_{N_f}\right)}{\Delta t_{N_1\_fic}\left(x_{N_f}\right)}=\begin{cases}\dfrac{l_{N_cN_f}-x_{N_f}}{x_{N_f}+l_{N_1N_f}}, & 0<x_{N_f}\le\dfrac{l_{N_cN_f}-l_{N_1N_f}+l_{N_1N_c}}{2}\\ \dfrac{l_{N_cN_f}-x_{N_f}}{l_{N_cN_f}-x_{N_f}+l_{N_1N_c}}, & \dfrac{l_{N_cN_f}-l_{N_1N_f}+l_{N_1N_c}}{2}<x_{N_f}\le l_{N_cN_f}\end{cases}\tag{15}$$

Else if $l_{N1Nc}+l_{NcNf}\le l_{N1Nf}$ and $l_{N1Nc}+l_{N1Nf}<l_{NcNf}$, then we have:

$$R_{N_cN_1\_fic}\left(x_{N_f}\right)=\frac{\Delta t_{N_c\_fic}\left(x_{N_f}\right)}{\Delta t_{N_1\_fic}\left(x_{N_f}\right)}=\begin{cases}\dfrac{x_{N_f}+l_{N_1N_f}+l_{N_1N_c}}{x_{N_f}+l_{N_1N_f}}, & 0\le x_{N_f}\le\dfrac{l_{N_cN_f}-l_{N_1N_f}-l_{N_1N_c}}{2}\\ \dfrac{l_{N_cN_f}-x_{N_f}}{x_{N_f}+l_{N_1N_f}}, & \dfrac{l_{N_cN_f}-l_{N_1N_f}-l_{N_1N_c}}{2}<x_{N_f}\le l_{N_cN_f}\end{cases}\tag{16}$$

Else, we have:

$$R_{N_cN_1\_fic}\left(x_{N_f}\right)=\frac{\Delta t_{N_c\_fic}\left(x_{N_f}\right)}{\Delta t_{N_1\_fic}\left(x_{N_f}\right)}=\frac{l_{N_cN_f}-x_{N_f}}{l_{N_cN_f}-x_{N_f}+l_{N_1N_c}}\tag{17}$$

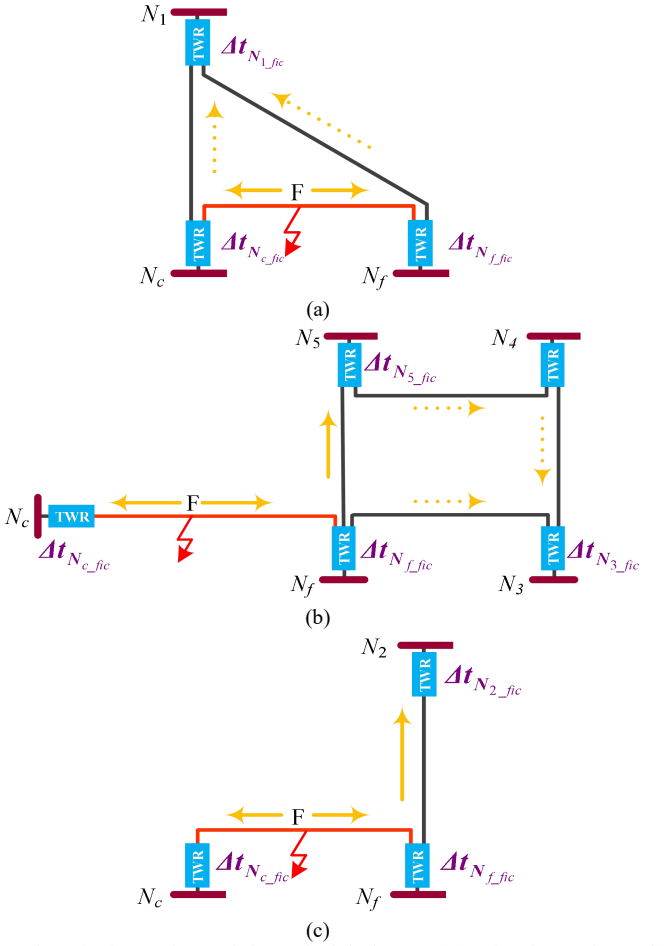


Fig.3 Three basic topology of the typical fault area. (a) Triangle topology, (b) Loop topology and (c) Radial topology

### C. FL Objective Function Solution by Equal-interval Search Algorithm

Equal-interval search algorithm is employed to solve (13). The basic principle of equal-interval search algorithm is simply illustrated in Fig.4. In the figure, the line between bus $N_f$ and $N_c$ is the detected fault line whose length is $L_F$. The actual fault point $F$ is $x_r$ away from bus $N_F$. The determined fault range by (12) is $x_{c\_min}$ ~ $x_{c\_max}$. First, the computation interval $[a,b]$ can be determined as: $a=x_{c\_min}$ and $b=x_{c\_max}$. Next, let $x_1=a+0.25(b-a)$, $x_2=a+0.5(b-a)$, $x_3=a+0.75(b-a)$, and the $f(x_1)$, $f(x_2)$ and $f(x_3)$ are calculated. Then, the values of $f(x_1)$, $f(x_2)$ and $f(x_3)$ are compared. If $f(x_1)>f(x_2)>f(x_3)$, a new computation interval $[a,b]$ is determined as: $a=x_2$, b= $x_{c\_max}$, and let $x_1=a+0.25(b-a)$, $x_2=x_3$, $x_3=a+0.75(b-a)$; Else if $f(x_1)<f(x_2)<f(x_3)$, a new computation interval $[a,b]$ can be determined as: $a=x_{c\_min}$, $b=x_2$, and let $x_1=a+0.25(b-a)$, $x_2=x_1$, $x_3=a+0.75(b-a)$; Else, a new computation interval $[a,b]$ is determined as: $a=x_1$, $b=x_3$, and let $x_1=a+0.25(b-a)$, $x_2=x_2$, $x_3=a+0.75(b-a)$. Last, the steps mentioned above are repeated until $|b-a|<\theta$ and $x_r=0.5(a+b)$ when searching the minimum value of $f(x_F)$.

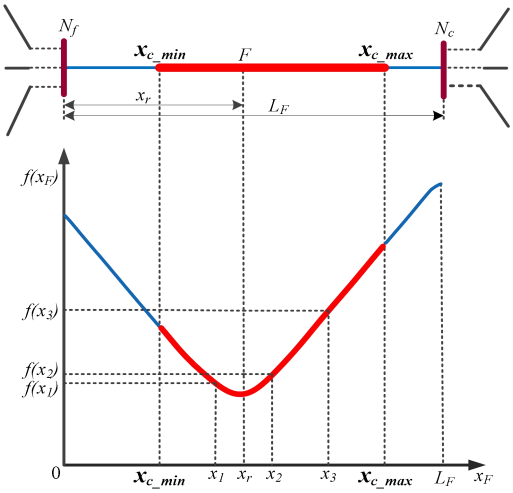


Fig.4 The curve of the FL objective function

## IV. SIMULATION TEST

In order to validate the proposed FL scheme, various faults with different fault impedances, inception angles, locations were simulated by PSCAD/EMTDC in the IEEE 30-bus [19] test system shown in Fig.5. The sampling rate in simulation is 1MHz. The proposed FL scheme was carried out in MATLAB. A universal FL error $e$ is defined in [20].

### A. Case Study

In order to verify the effectiveness of the proposed fault location scheme, two typical single-phase-to-earth faults are simulated in the line between bus 10 and 17 whose length is 116km ($L_F$=116km). The fault impedances and inception angles of the two faults are 200Ω and 30°, respectively. The first and

This article has been accepted for publication in a future issue of this journal, but has not been fully edited. Content may change prior to final publication. Citation information: DOI 10.1109/TII.2019.2903267, IEEE Transactions on Industrial Informatics

second faults (classified as general and near-bus faults respectively) are 65km and 114km away from bus 17, respectively. For the general and near-bus faults, the actual TDOA information of the MTWs measured at each bus is listed in TABLE 1. According to the proposed fault area determination criterion, bus 10 is closest to the actual fault point in both of the two faults.

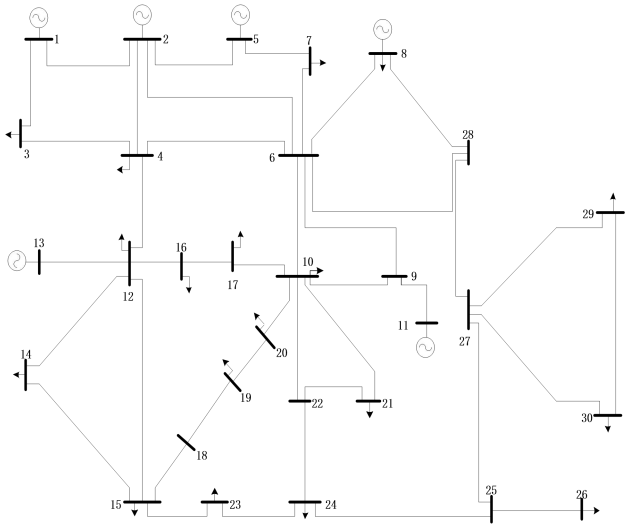

Fig.5 Single line diagram of IEEE30-bus test system

TABLE 1. ACTUAL TDOA AT EACH BUS FOR THE TWO TYPICAL FAULTS

(A) ACTUAL TDOA AT EACH BUS FOR THE GENERAL FAULT

| Bus | No.1 | No.2 | No.3 | No.4 | No.5 | No.6 |
|---|---|---|---|---|---|---|
| TDOA(μs) | 452 | 76 | 62 | 46 | 66 | 32 |
| Bus | No.7 | No.8 | No.9 | No.10 | No.11 | No.12 |
| TDOA(μs) | 36 | 64 | 18 | 3 | 28 | 44 |
| Bus | No.13 | No.14 | No.15 | No.16 | No.17 | No.18 |
| TDOA(μs) | 82 | 90 | 100 | 32 | 8 | 94 |
| Bus | No.19 | No.20 | No.21 | No.22 | No.23 | No.24 |
| TDOA(μs) | 42 | 14 | 32 | 34 | 100 | 66 |
| Bus | No.25 | No.26 | No.27 | No.28 | No.29 | No.30 |
| TDOA(μs) | 117 | 156 | 92 | 54 | 154 | 140 |

(B) ACTUAL TDOA AT EACH BUS FOR THE NEAR-BUS FAULT

| Bus | No.1 | No.2 | No.3 | No.4 | No.5 | No.6 |
|---|---|---|---|---|---|---|
| TDOA(μs) | 26 | 66 | 134 | 148 | 55 | 22 |
| Bus | No.7 | No.8 | No.9 | No.10 | No.11 | No.12 |
| TDOA(μs) | 32 | 57 | 12 | 1 | 22 | 48 |
| Bus | No.13 | No.14 | No.15 | No.16 | No.17 | No.18 |
| TDOA(μs) | 49 | 98 | 102 | 36 | 13 | 86 |
| Bus | No.19 | No.20 | No.21 | No.22 | No.23 | No.24 |
| TDOA(μs) | 38 | 10 | 23 | 20 | 188 | 58 |
| Bus | No.25 | No.26 | No.27 | No.28 | No.29 | No.30 |
| TDOA(μs) | 116 | 150 | 84 | 46 | 148 | 132 |

Based on the fictitious fault point method, a fictitious fault point is moving along the line section between bus $N_i$ and $N_j$, which belongs to {6, 9, 17, 20, 21, 22}. In each fault simulation, the accumulated equivalent absolute difference of the line section between buses $N_i$ and $N_j$ is listed in TABLE 2, where $D_{acc\_equ}$ and $L_{Ni}$ respectively represent the corresponding difference and the line section between buses $N_i$ and $N_j$. $x_{min\_max}$ represents the minimum and maximum FLs determined by using the TDOA of $L_{Ni}$. It is abundantly clear that the bus corresponding to the minimum $D_{acc\_equ}$ is the other terminal bus of the fault line. Thus, for the two fault simulations, the line between bus **10** and **17** is detected as the fault line according to the calculation results in TABLE 2.

TABLE 2. ACCUMULATED EQUIVALENT ABSOLUTE DIFFERENCE AND FL RANGES FOR THE TWO TYPICAL FAULTS

(A) ACCUMULATED EQUIVALENT ABSOLUTE DIFFERENCE AND FL RANGES FOR THE GENERAL FAULT

| Line section | $L_6$ | $L_9$ | $L_{17}$ |
|---|---|---|---|
| $D_{acc\_equ}$ | 3.2185 | 1.7341 | **0.1685** |
| Line section | $L_{20}$ | $L_{21}$ | $L_{22}$ |
| $D_{acc\_equ}$ | 1.5901 | 2.4030 | 2.9160 |
| Data source | Bus 17-6 | Bus 17-9 | Bus 17-10 |
| $x_{min\_max}$ (km) | (**49.176**, 63.226) | (57.078, 73.386) | (73.819, 94.910) |
| Data source | Bus 17-20 | Bus 17-21 | Bus 17-22 |
| $x_{min\_max}$ (km) | (57.592, 74.046) | (58.801, **75.601**) | (53.334, 68.572) |

(B) ACCUMULATED EQUIVALENT ABSOLUTE DIFFERENCE AND FL RANGES FOR THE NEAR-BUS FAULT

| Line section | $L_6$ | $L_9$ | $L_{17}$ |
|---|---|---|---|
| $D_{acc\_equ}$ | 1.2684 | 0.5569 | **0.4543** |
| Line section | $L_{20}$ | $L_{21}$ | $L_{22}$ |
| $D_{acc\_equ}$ | 0.4859 | 0.7096 | 0.5956 |
| Data source | Bus 17-6 | Bus 17-9 | Bus 17-10 |
| $x_{min\_max}$ (km) | (**96.344**, 112.401) | (101.761, 114.834) | **abandoned** |
| Data source | Bus 17-20 | Bus 17-21 | Bus 17-22 |
| $x_{min\_max}$ (km) | (98.728, **116**) | (112.001, **116**) | (**116**, **116**) |

TABLE 2 also shows the FL ranges (maximum and minimum calculated FLs) determined by using the TDOA of each line section that contains the detected fault line. As for the general fault, the longest calculated fault distance is 75.601km. $|L_F - x_{c\_max}|$= |116−75.601|km= 40.399km >5km, thus the TDOA of the MTWs acquired at bus 10 can be utilized. As for the near—bus fault, the longest calculated fault distance is 116km ($x_{c\_max}$=116km). Since $|L_F - x_{c\_max}|$=|116−116|km=0km<5km, the TDOA information of the MTWs acquired at bus 10 cannot be utilized. Thus, in TABLE 2 (B), the data from bus 17-10 is

This article has been accepted for publication in a future issue of this journal, but has not been fully edited. Content may change prior to final publication. Citation information: DOI 10.1109/TII.2019.2903267, IEEE Transactions on Industrial Informatics

abandoned. In addition, the FL objective function curves for the two faults are depicted in Fig.6. By using the equal-interval search algorithm, the accurate FLs of the two faults can be obtained. From the figure, it can be observed that the FL errors of the two faults are only |65km−65.233km|/116km =0.2% and |114km−114.156km |/116km =0.13%, respectively. The final FL calculated by solving the FL objective function in (13) is far below the ones obtained in fault line detection.

### *B. Robustness Analysis*

#### *1) Fault Distances, Impedance and Inception Angles Effects*

The performance of the FL scheme is evaluated under different fault impedances and inception angles. Various single-phase-to-earth faults with different fault impedances (10Ω and 200Ω) and fault inception angles (30° and 90°) are simulated in the line between buses 4 and 6 (denoted as $L_{4\text{-}6}$). The total length of the line is 112km. The FL results are shown in Table 3, where the fault distance is the distance between the calculated FL and bus 4. It can be seen from the table that the FL error grows with the increase of fault impedances. The FL error is the largest when the fault inception angle is 30°. The fault line detection is not influenced by fault impedance and inception angles to a certain extent. The FL errors under high fault impedances and small inception angle mainly result from the inaccurate extraction of TDOA information of the MTWs. Although the FL error varies with fault impedances and inception angles, the largest error is lower than 0.18% in these cases.

TABLE 3. FL RESULTS WITH DIFFERENT FAULT CONDITIONS

| Fault Distance (km) | Fault Impedance (Ω) | Inception Angle (°) | Fault Line Detection | *e* (%) |
|---|---|---|---|---|
| 4 | 10 | 30 | $L_{4\text{-}6}$ | 0.122 |
| | | 90 | $L_{4\text{-}6}$ | 0.104 |
| | 200 | 30 | $L_{4\text{-}6}$ | 0.131 |
| | | 90 | $L_{4\text{-}6}$ | 0.117 |
| 55 | 10 | 30 | $L_{4\text{-}6}$ | 0.165 |
| | | 90 | $L_{4\text{-}6}$ | 0.146 |
| | 200 | 30 | $L_{4\text{-}6}$ | 0.172 |
| | | 90 | $L_{4\text{-}6}$ | 0.158 |
| 108 | 10 | 30 | $L_{4\text{-}6}$ | 0.131 |
| | | 90 | $L_{4\text{-}6}$ | 0.123 |
| | 200 | 30 | $L_{4\text{-}6}$ | 0.154 |
| | | 90 | $L_{4\text{-}6}$ | 0.143 |

#### *2) Noise Effect*

In actual FL practices, the measured MTW signals can easily get contaminated with noises, which results in inaccurate detection of the arrival time stamps of the traveling wave signals. In order to investigate the impact of noise interference on the performance of the proposed FL scheme, white Gaussian noises with different signal-to-noise ratios (SNRs) are added to the recorded MTW signals at each bus node after a single-phase-to-earth fault is simulated in the line between buses 12 and 15. The fault occurs at 0.08s and the fault impedance is 200Ω. The FL results of the fault line between bus 12 and 15 under five different levels of noise interference (SNR=80, 85, 90, 95, 100) are displayed in Fig.7. In the figure, the fault distance is the distance from bus 15. From the figure, one can conclude that the FL error increases with the decrease of SNR values and the largest FL error does not exceed 0.25% in different cases.

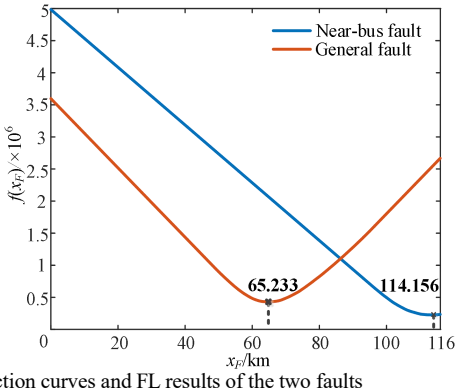


Fig.6 FL function curves and FL results of the two faults

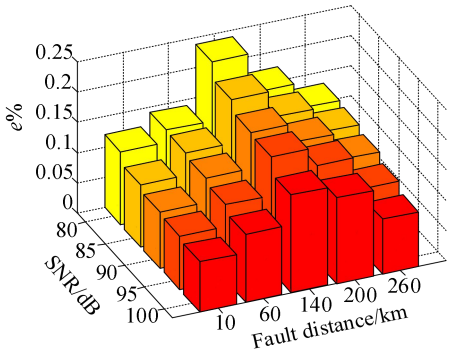


Fig.7 FL results under different noise interference levels

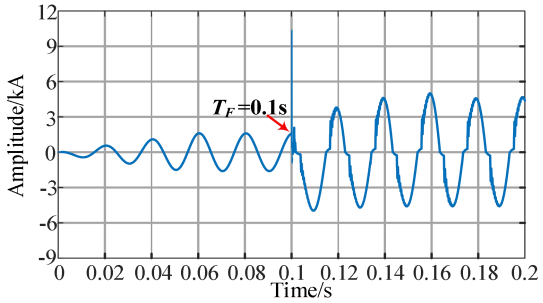


Fig.8 Current waveform of the simulated arc

#### *3) Arc Effect*

To investigate the effect of arc on the proposed method, the single-phase arc grounding faults are simulated at different locations in two lines in IEEE-30 bus system. The model of arc used in simulations is based on the work of [22]. The current waveform of the simulated arc is shown in Fig.8. In the figure, $T_f$ =0.1s is the fault occurrence time set in simulation. The FL errors

This article has been accepted for publication in a future issue of this journal, but has not been fully edited. Content may change prior to final publication. Citation information: DOI 10.1109/TII.2019.2903267, IEEE Transactions on Industrial Informatics

with different fault distance percentages are included in Fig.9. It can be observed that the minimum and maximum FL errors with arc faults are about 0.062% and 0.197%, respectively, which are close to the simulation results with ordinary faults. In summary, arc has no significant impact on the proposed FL scheme.

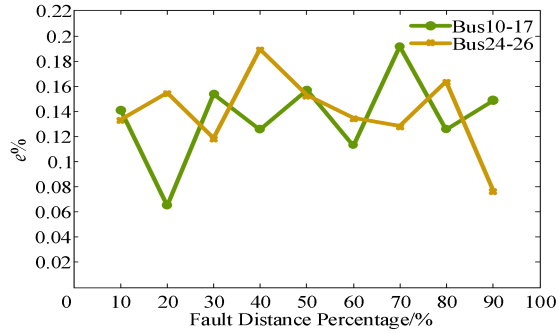


Fig.9 FL results with arc fault

## C. Comparison Work

### 1) Comparison with the Traditional Methods to Calculated the TDOA Ratio $R_{NiNj\_fic}$

To show the high efficiency of the proposed method in calculating $R_{NiNj\_fic}$, a comparison between the proposed method and three traditional methods (Dijkstra, Floyd and Bellman-ford algorithms) is performed. A single-phase-to-earth fault with 200Ω fault impedance and 30° fault inception angle is simulated in the line between bus 10 and 17. All the computations are carried out in a computer whose processor is Intel Core(TM) i5-6300HQ @ 2.30 Hz. By using the operation time measurement functions *tic* and *toc* in MATLAB, the total time of computing $R_{NiNj\_fic}$ (for one line section) by the proposed method and the other three methods is determined and listed in TABLE 4. It can be observed that the proposed method calculates $R_{NiNj\_fic}$ with the highest speed (only 4.54ms) while the least time taken for the other algprithms is 16.17ms. Thus, the proposed method can effecitvely reduce the time of computing $R_{NiNj\_fic}$ to some extent.

TABLE 4. COMPUTATION TIME OF TDOA RATIO BY FOUR METHODS

| Algorithm | Dijkstra | Floyd | Bellman-ford | Proposed method |
|---|---|---|---|---|
| Time (ms) | 21.82 | 16.17 | 33.68 | 4.51 |

### 2) Comparison with the State-of-the-art FL Methods

To demonstrate the superiority of the proposed FL scheme, a comparison between the proposed FL method and four most-state-of-the-art traveling wave based FL methods is conducted and the results are listed in TABLE 5. From TABLE 5, the method in [19] needs the knowledge of TDOA while all the other methods do not, which means that only the method in [19] requires a large data set. The methods in [9], [14], [21] need the information of the traveling wave velocity but the others do not. In actual FL practices, noises have important impacts on the detection of arrival time of MTWs. The method in [19] and the proposed method are validated with noise inference, but the noise effects are not considered in the other methods. The proposed method considers the near-bus fault with only 2km fault distance, but this special case is not mentioned in the remaining methods. In addition, only the methods in [9] and [14] depend on synchronous measurements. In conclusion, the proposed method has the advantages of asynchronous measurement, no need of prior knowledge and adaptability to both general and near-bus faults.

TABLE 5. COMPARISON WITH SEVERAL FL METHODS

| Methods | Topology | Wave velocity | Synchronization | Knowledge | Anti-noise ability | Near-bus fault | Average FL error (%) |
|---|---|---|---|---|---|---|---|
| [9] | IEEE30 | Yes | Yes | No | Not considered | Not mentioned | 0.54 |
| [14] | IEEE30 | Yes | Yes | No | Not considered | Not mentioned | 0.13 |
| [19] | IEEE30 | No | No | Yes | SNR=50dB | Not mentioned | 0.14 |
| [21] | 6-bus | Yes | No | No | Not considered | Not mentioned | 0.75 |
| Proposed method | IEEE30 | No | No | No | SNR=80dB | 2km | 0.14 |

## V. CONCLUSIONS

A novel FL scheme using the TDOA of MTWs is developed for power networks. The TDOAs of the MTWs asynchronously sampled at buses are used to determine the fault area. Considering the propagation path and network topology, the equivalent difference between the calculated and fictitious TDOA ratio is used to estimate the accurate FL. In accurate FL, by determining the rough FL, the TDOA of the MTWs measured at adjacent buses is fully used, which effectively improves the FL accuracy for both the general and near-bus faults. The proposed FL scheme does not need synchronous measurement, wave velocity and priori knowledge. The robustness of the scheme to noise interference is also validated. The future work of our research is focused on FL in distribution networks with traveling wave information.

## REFERENCES

[1] Xiaowei Wang, Jie Gao , Mingfei Chen, et al. “Faulty Line Detection Method Based on Optimized Bistable System for Distribution Network,” *IEEE Trans. Industrial Informatics*, vol.14, no.4, pp:1370-1381, 2018.

[2] Pratim Kundu and Ashok Kumar Pradhan. “Real-Time Analysis of Power System Protection Schemes Using Synchronized Data,” *IEEE Trans. Industrial Informatics*, vol.14, no.9, pp:3831-3839, 2018.

[3] Spoor Darren, Zhu Jian Guo. “Improved single-ended traveling wave fault location algorithm based on experience with conventional substation transducers,” *IEEE Trans. Power Delivery*, vol.21, no.3, pp:1714–20, 2006.

[4] Ning Kang, Yuan Liao. “Double-Circuit Transmission-Line Fault Location With the Availability of Limited Voltage Measurements,” *IEEE Trans. Power Delivery*, vol. 27, no.1, pp:325–336, 2012.

[5] Xiangning Lin, Feng Zhao, Gang Wu, Zhengtian Li, and Hanli Weng. "Universal Wavefront Positioning Correction Method on Traveling-Wave-Based Fault-Location Algorithms," *IEEE Trans. Power Delivery*, vol. 27, no. 3, pp:1601–1610, 2012.

[6] Yanhui Xi, Zewen Li, Xiangjun Zeng, et al. "Fault location based on travelling wave identification using an adaptive extended Kalman filter," *IET Generation, Transmission & Distribution*, vol.12, no.6, pp: 1314-1322, 2018.

[7] Guangbin Zhang, Hongchun Shu, Yuan Liao. "Automated double-ended traveling wave record correlation for transmission line disturbance analysis," *International Journal of Electrical Power Systems Research*, vol.136, pp:242–250, 2016.

[8] D. Spoor, Jianguo Zhu. "Improved single-ended traveling-wave fault-location algorithm based on experience with conventional substation transducers," *IEEE Trans. Power Delivery*, vol. 21, no.3, pp:1714-1720, 2006.

[9] Mert Korkali, Hanoch Lev-Ari, Ali Abur. "Traveling-Wave-Based Fault-Location Technique for Transmission Grids Via Wide-Area Synchronized Voltage Measurements," *IEEE Trans. Power Systems*, vol. 27, no.2, pp:1003 – 1011, 2012.

[10] Mert Korkali, Ali Abur. "Optimal Deployment of Wide-Area Synchronized Measurements for Fault-Location Observability," *IEEE Trans. Power Systems*, vol.28, no.1, pp:482 – 489, 2013.

[11] Yongli Zhu, Xinqiao Fan. "Fault location scheme for a multi-terminal transmission line based on current traveling waves," *International Journal of Electrical Power & Energy Systems*, vol.53, no.1, pp:367–374, 2013.

[12] Yu Chen, Dong Liu, Bingyin Xu. "A traveling wave location algorithm based on wide area network information," *Automation of Electric Power Systems*, vol.35, no.11, pp:65–70, 2011.

[13] Mert Korkalı, Ali Abur. "Robust Fault Location Using Least-Absolute-Value Estimator," *IEEE Trans. Power Systems*, vol.28, no.4, pp:4384-4392, 2013.

[14] Rui Liang, Fei Wang, Guoqing Fu, Xue Xue, Rui Zhou. "A general fault location method in complex power grid based on wide-area traveling wave data acquisition," *International Journal of Electrical Power & Energy Systems*, vol.83, pp:213–218, 2016.

[15] Zewen Li, Jiangang Yao, Xiangjun Zeng, et al. "Fault location based on traveling wave time difference in power grid," *Proceedings of CSEE*, vol. 29, no.4, pp:60–64, 2009.

[16] Zewen Li, Xiangjun Zeng, Jiangang Yao, Xianghui Chu, Feng Deng. "Wide area traveling wave based power grid fault network location method," *International Journal of Electrical Power & Energy Systems*, vol. 63, no.63 , pp:173-177,2014.

[17] Yu Chen, Dong Liu, Bingyin Xu. "Wide-area traveling wave fault location system based on IEC61850," *IEEE Trans. Smart Grid*, vol.4, no.2, pp:1207–1215, 2013.

[18] Pulin Cao, Hongchun Shu , Bo Yang, Jun Dong, Yi Fang, Tao Yu. "Speeded-up robust features based single-ended travelling wave fault location: a practical case study in Yunnan power grid of China," *IET Generation, Transmission & Distribution*, vol.12, no.4, pp: 886–894, 2018.

[19] Rui Liang, Chenglei Liu, Nan Peng, Menghan Cheng, Fei Wang. "Fault location for power grid based on transient travelling wave data fusion via asynchronous voltage measurements," *International Journal of Electrical Power & Energy Systems*, vol.93, no.12, pp: 426-439, 2017.

[20] M.da Silva, D.V. Coury, M. Oleskovicz, E.C. Segatto. "Combined solution for fault location in three-terminal lines based on wavelet transforms," *IET Generation, Transmission & Distribution*, vol.4, no.1, pp:94-103, 2010.

[21] Xiaopeng Li, Zhengyou He, Lulu Xia. "A novel fault location method using traveling wave natural frequencies for transmission grid," presented at the 4th Int. Conf. on Electric Utility Deregulation and Restructuring and Power Technologies, Shandong, China, Jul. 209-212, 2011.

[22] Renato G. Ferraz, Leonardo U. Iurinic, André D. Filomena, et al. "Arc fault location: A nonlinear time varying fault model and frequency domain parameter estimation approach," *International Journal of Electrical Power & Energy Systems*, vol. 80, pp: 347-335.